

STUDY ON THE ACCELERATED CORROSION BEHAVIOR OF A GALVANIZED X80 PIPELINE STEEL WELDED JOINT DURING A CYCLIC SALT SPRAY TEST

ŠTUDIJA POSPEŠENE KOROZIJE ZVARNIH SPOJEV GALVANIZIRANEGA JEKLA ZA CEVI X80 V POGOJIH PREIZKUŠANJA Z IZMENIČNIM NAPRŠEVANJEM S SLANICO

Mengmeng Li¹, Hongchao Ji^{1,2*}, Chun Han³, Shengqiang Liu², Wenchao Xiao⁴

¹College of Mechanical Engineering, North China University of Science and Technology, Tangshan 063210 China

²School of Materials Science and Engineering, Zhejiang University, Hangzhou 310030, China

³China 22 MCC Group Corporation Limited, Hebei, Tangshan 063035

⁴Shenzhen Institute for Advanced Study, University of Electronic Science and Technology of China, Guangdong, Shenzhen 518000, China

Prejem rokopisa – received: 2023-10-24; sprejem za objavo – accepted for publication: 2023-10-20

doi:10.17222/mit.2023.946

The corrosion behavior of galvanized X80 pipeline steel welded joints in a marine atmospheric environment was studied using the cyclic salt spray accelerated corrosion test. The corrosion weight loss, corrosion morphology and corrosion products of samples under different cycles were characterized by means of appearance inspection, SEM and EDS. The results show that with the rupture of the galvanized layer, cracks first appear when the weld metal is exposed for eight days. With the infiltration of the corrosive liquid, pitting pits first appear in the weld metal. In the early stage of corrosion in the heat-affected zone, the fracture degree of the zinc layer is more serious than that in the other two areas. The corrosion products of the zinc layer accumulate irregularly and more pits appear, resulting in early cracks and pitting pits in the later stage. Compared with the first two regions, the base metal shows better corrosion resistance.

Keywords: galvanized alloy steel, X80 pipeline steel, corrosion of welded joints, cyclic salt spray test

V članku je opisan potek pospešene korozije zvarnih spojev legiranega jekla za cevi vrste X80 s pomočjo korozijskega preizkusa izmeničnega naprševanja s slanico, ki simulira atmosferske pogoje na morju oziroma izpostavljenost koroziji plovil med plovbo po morju. Avtorji so izvedli meritve izgub na masi, analizo morfologije korozijskih produktov, vizualne teste in karakterizacijo na vzorcih s pomočjo vrstične elektronske mikroskopije in mikrokemijskih analiz (SEM/EDS). Rezultati kažejo, da se po porušitvi galvanizirane plasti razpoke pojavijo po 8 dneh izvajanja preizkusov izmeničnega naprševanja. Z infiltracijo korozivne kapljevine se korozijske jamice pojavijo najprej na zvarih. V zgodnjem stadiju korozije je plast cinka nad toplotno vplivano cono mnogo bolj poškodovana kot v ostalih dveh področjih (osnovni kovini in kovini za varjenje oziroma področje staljenega dela zvara). Korozijski produkti plasti cinka se nabirajo neenakomerno, pojavljajo se korozijske jamice, kar vodi do zgodnje tvorbe več razpok in korozijskih jamic v kasnejših stadijih korozije. Medsebojna primerjava prvih dveh področij kaže, da ima osnovna kovina boljšo odpornost proti koroziji.

Ključne besede: galvanizirano legirano jeklo, jeklo za cevovode vrste X80, korozija zvarnih spojev, ciklični test naprševanja s slanico

1 INTRODUCTION

In order to carry out efficient transportation of oil and natural gas, we have higher expectations regarding the performance of pipeline steel. It should exhibit not only high strength and toughness, but also greater thickness and diameter. As a high-strength low-alloy steel, X80 pipeline steel is widely used in oil and gas transportation¹⁻³ because it can withstand the large pressure generated inside a pipeline. Welding is an important processing technology in pipeline production and laying. The main welding processes currently used are submerged arc welding and gas shielded welding. In the process of pipeline transportation, the corrosion of pipeline steel needs special attention^{4,5} and the corrosion of pipeline steel welded joints is one of the key issues.⁶ Welded

joints mainly consist of the heat-affected zone (HAZ), weld metal (WM) and base metal (BM). The heterogeneous microstructure and residual stress between these regions vary significantly, resulting in different corrosion behaviors of welded joints.⁷ Many methods have been used to prevent the corrosion of low carbon steel, including painting, anodizing and chemical conversion coatings.⁸

Zinc and zinc-aluminum materials are often used as sacrificial anode coatings to protect alloy steel substrates due to their high chemical activity and low price. The service life of zinc-coated steel can be as long as several decades because a zinc coating greatly improves the corrosion resistance of steel products exposed to corrosive environments.⁹ A zinc coating protects the underlying carbon steel substrate by forming a passivation layer, simultaneously providing a sacrificial anode. The zinc coating has a more negative corrosion potential than the

*Corresponding author's e-mail:
jihongchao@ncst.edu.cn (Hongchao Ji)

steel substrate. During a corrosion process, the zinc coating preferentially corrodes and acts as an anode, which contributes to the corrosion inhibition of the steel substrate. The corrosion of galvanized steel occurs in three steps. First, corrosion occurs due to the dissolution of the zinc coating, and then corrosion products are formed, thereby reducing the overall corrosion rate of the zinc coating. In the second stage, after the local consumption of the zinc coating, the steel substrate is corroded. In the final stage, the zinc coating is completely consumed, and the bare steel substrate is corroded down to the carbon steel, covered with corrosion products.¹⁰

With the increasing demand for oil and gas energy around the world, the exploration, exploitation and transportation of oil and gas from unconventional fields (such as basins, oceans, etc.) have attracted more and more attention. However, there are few studies on the corrosion of galvanized X80 pipeline steel welded joints in a marine atmospheric environment. Previous studies focused on the corrosion of X80 pipeline steel welded joints in conventional oil and gas environments^{11,12} or the corrosion of X80 pipeline steel in unconventional oil and gas environments.^{13,14}

Igor et al.⁷ found that pitting corrosion in the heat-affected zone is more serious than that in the weld or base metal. Persson et al.⁹ found that corrosion products containing sulfates and chlorides ($Zn(OH)_2 \cdot 3ZnSO_4 \cdot nH_2O$, $NaZn_4(SO_4)(OH)_6Cl \cdot 6H_2O$ and $Zn_5(OH)_8Cl_2 \cdot H_2O$ were formed at the anode of a corrosion pit, and $Zn_5(OH)_6(CO_3)_2$ was mainly formed on the outside of the corrosion product and the cathode area of the corrosion pit. Corrosion of galvanized steel usually begins with localized corrosion.¹⁵ Wang et al.¹⁶ found that when there is a zinc layer on a weld interface, the total electrochemical corrosion performance of the welded joint is improved. The presence of the zinc layer can reduce the corrosion rate and improve the strength of the weld.

In addition, the corrosion products of zinc coatings usually have complex structures and a lower conductivity, which can greatly reduce the electron transport during the electrochemical corrosion reaction and/or physically prevent the migration of corrosion ions to the underlying substrate. Therefore, the chemical and physical properties of a zinc coating and its corrosion products have always made galvanized steel one of the most commonly used structural materials.

In this study, based on an accelerated corrosion test of simulating the effect of a marine atmospheric environment, the corrosion behavior of galvanized X80 pipeline steel and its welded joints was characterized using a cyclic salt spray accelerated corrosion test, corrosion weight loss analysis and scanning electron microscopy.

The corrosion behavior of galvanized X80 pipeline steel and its welded joints was characterized by corrosion kinetics, morphology and composition of corrosion products. The study provides a theoretical basis for pipeline protection measures, improving the corrosion resistance of weak areas of welded joints, ensuring a safe transportation and improving the transportation efficiency.

2 EXPERIMENTAL PART

2.1 Material and specimen preparation

The test sample is X80 pipeline steel with a galvanized layer on the surface, and **Table 1** shows the chemical composition of X80 pipeline steel.

In the process of sample preparation, the X80 pipeline steel plate was first cut into (50 × 18.4 × 10) mm samples. The surfaces of the samples were successively polished with 120–2000# water-grinding sandpaper until there were no defects such as scratches on them. Surface oil and impurities of the samples were cleaned with anhydrous ethanol and the samples were dried in a dry hot airflow. The samples were then weighed using an electronic scale (accurate to 0.01 mg). Secondly, the surface of the X80 pipeline steel was electroplated and the galvanized pipeline steel was weighed; the weighing was also accurate to 0.01 mg. Finally, in accordance with 'GB/T 10125-2012: Corrosion tests in artificial atmospheres – Salt spray tests', a test was carried out in a programmable salt spray test chamber.

2.2 Accelerated corrosion test

In this experiment, the acid salt spray dry-wet cycle accelerated corrosion method was used. The test conditions were as follows: (a) The salt spray composition was (5 ± 0.5)%NaCl; (b) Salt spray process: the nozzle pressure was 80 kPa, the spray temperature was (3 ± 0.5) °C; (c) Drying process: the temperature was (60 ± 1) °C, RH < 30 %; (d) Cycle period: an alternating experiment was carried out including 8 h of spraying + 16 h of drying per cycle (1 d), and (4, 8, 16, 24, 32 and 40) cycles were completed. Sampling and corrosion performance testing were carried out at the test nodes after (4, 8, 16, 24, 32 and 40) d, respectively, in order to grasp the corrosion behavior and corrosion damage of the material.

2.3 Corrosion performance test

During the test, three test samples with corrosion products were regularly taken out; two of them were used for a corrosion weight loss analysis, and one was processed into several small test pieces by wire cutting for a morphology and composition analysis.

Table 1: Chemical composition of X80 pipeline steel

| Chemical composition | C | Si | Mn | P | S | Cr | Ni | V | Ti | Mo | Nb |
|----------------------|--------|------|------|-------|--------|------|-------|-------|-------|------|-----|
| w/% | 0.0062 | 0.28 | 1.85 | 0.011 | 0.0006 | 0.03 | 0.016 | 0.059 | 0.016 | 0.22 | 0.1 |

Table 2: Corrosion data for galvanized X80 pipeline steel welded joints exposed to an accelerated corrosion environment for different times

| Exposure time | | 0 d | 4 d | 8 d | 16 d | 24 d | 32 d | 40 d |
|---------------|----------------------------------|-----|-------|-------|-------|-------|-------|-------|
| Sample 1 | Weight loss (g/cm ²) | 0 | 0.005 | 0.020 | 0.057 | 0.110 | 0.205 | 0.318 |
| | Corrosion rate (um/d) | 0 | 1.75 | 3.15 | 4.54 | 5.83 | 8.17 | 10.10 |
| Sample 2 | Weight loss (g/cm ²) | 0 | 0.005 | 0.016 | 0.047 | 0.095 | 0.163 | 0.236 |
| | Corrosion rate (um/d) | 0 | 1.75 | 2.62 | 3.76 | 5.01 | 6.47 | 7.51 |

2.3.1 Corrosion weight loss analysis

After removing the corrosion products, the mass loss ratio (ρ_m) and the corrosion rate (v) were calculated using the mass loss method, expressed by the following formulas:

$$\rho_m = \frac{m_0 - m_1}{m_1} \tag{1}$$

$$v = \frac{87600(m_0 - m_1)}{\rho S t} \tag{2}$$

where ρ_m is the ratio of the mass loss (%); m_0 is the mass of the uncorroded specimen (g); m_1 is the mass of the corroded sample after the rust removal (g); v is the corrosion rate ($\mu\text{m/d}$); ρ is the density of the material (g/cm^3); s is the surface exposed to the corrosive environment (cm^2); t is the corrosion time (h). In addition, the cross-sectional area of the parallel sample is the average of four equidistant cross-sectional areas in the corrosion area of the sample. The ratio of the cross-sectional area loss ΔA is defined as:

$$\Delta A = \frac{AV - A_1}{A_0} \tag{3}$$

where A_0 is the cross-sectional area (cm^2) of the parallel sample before corrosion, and A_1 is the cross-sectional area (cm^2) of the parallel sample after corrosion.

2.3.2 Corrosion morphology observation

The macroscopic morphology of a corrosion sample was observed using a digital camera, and the appearance inspection and macroscopic photography were performed. The surface morphology of the samples after

corrosion was observed with a metallographic microscope and scanning electron microscope (SEM), while the chemical composition of the corrosion products was analyzed with EDS and X-ray diffractometer (XRD). The determination was carried out with a SCIOS focused ion beam field emission scanning electron microscope produced in Czechia. The voltage was 20 kV and the current was 0.8 nA. The model of the X-ray diffractometer was APD2000PRO. The scanning range 2θ was $10\text{--}100^\circ$, the step width was 0.0° and the scanning rate was $10^\circ/\text{min}$.

3 RESULTS AND DISCUSSION

3.1 Corrosion kinetics

The data for the corrosion weight loss and corrosion rate of the samples exposed to an accelerated corrosion environment for different times are shown in **Table 2**, and the curve of the corrosion exposure time is shown in **Figure 1**. It can be seen from the corrosion weight loss and corrosion rate curves of the X80 pipeline steel exposed to an accelerated corrosion environment for different times that the accelerated corrosion exposure of X80 pipeline steel can be roughly divided into four stages. In the first stage (4–16 d), the trend of corrosion weight loss and corrosion rate increased slowly, indicating that the zinc layer had a good protective effect on the substrate at the initial stage of corrosion. In the second stage (16–24 d), the trend of corrosion weight loss and corrosion rate increased more slowly and the difference between the two groups was lower than that in the first stage. At this time, the zinc layer was locally corroded,

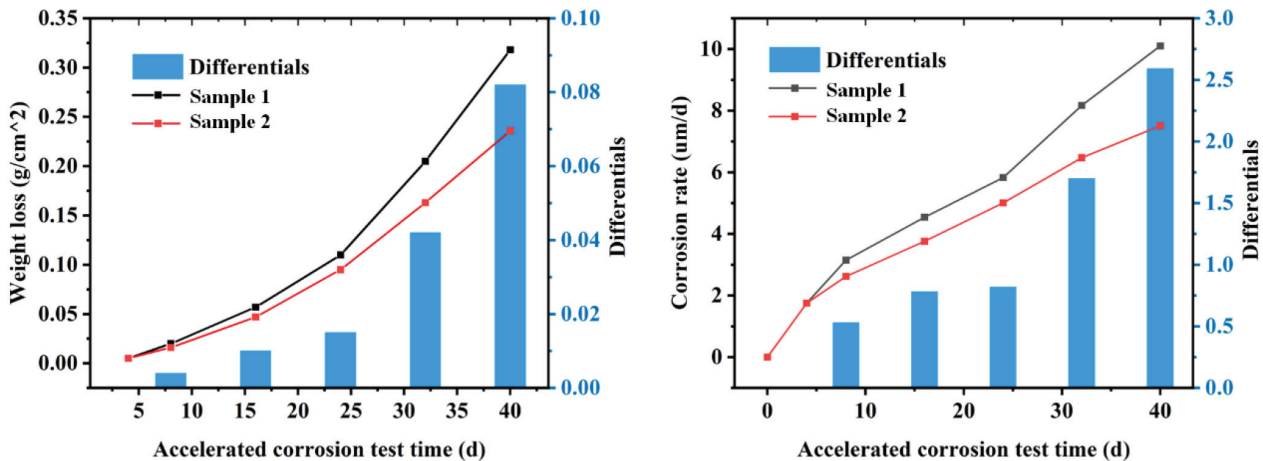


Figure 1: Corrosion weight loss curve and corrosion rate curve of galvanized X80 pipeline steel welded joints

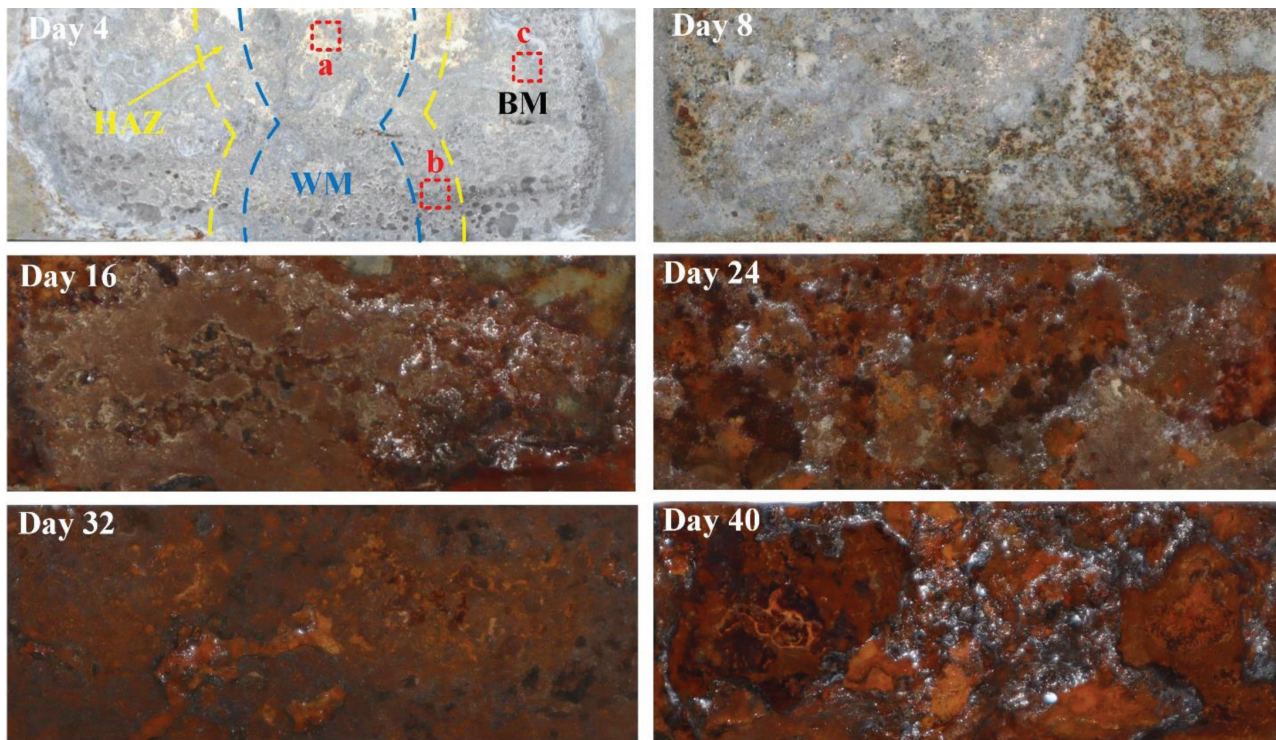


Figure 2: Macroscopic diagram and the measuring point of a galvanized X80 pipeline steel welded joint

and the corrosion products produced due to the exposed substrate were combined with the corrosion products of the galvanized layer, increasing the protection of the substrate. In the third stage (24–40 d), with the extension of the exposure time, the zinc layer on the surface of the substrate was completely corroded, and the surface rust layer began to loosen or even fall off. The unprotected substrate surface was affected by corrosive media such

as Cl^- and H^+ , resulting in a rapid increase in the corrosion weight loss and corrosion rate.

3.2 Corrosion morphology analysis

Figure 2 shows the macroscopic morphology of galvanized X80 pipeline steel exposed to an accelerated corrosion environment for different periods. By observing

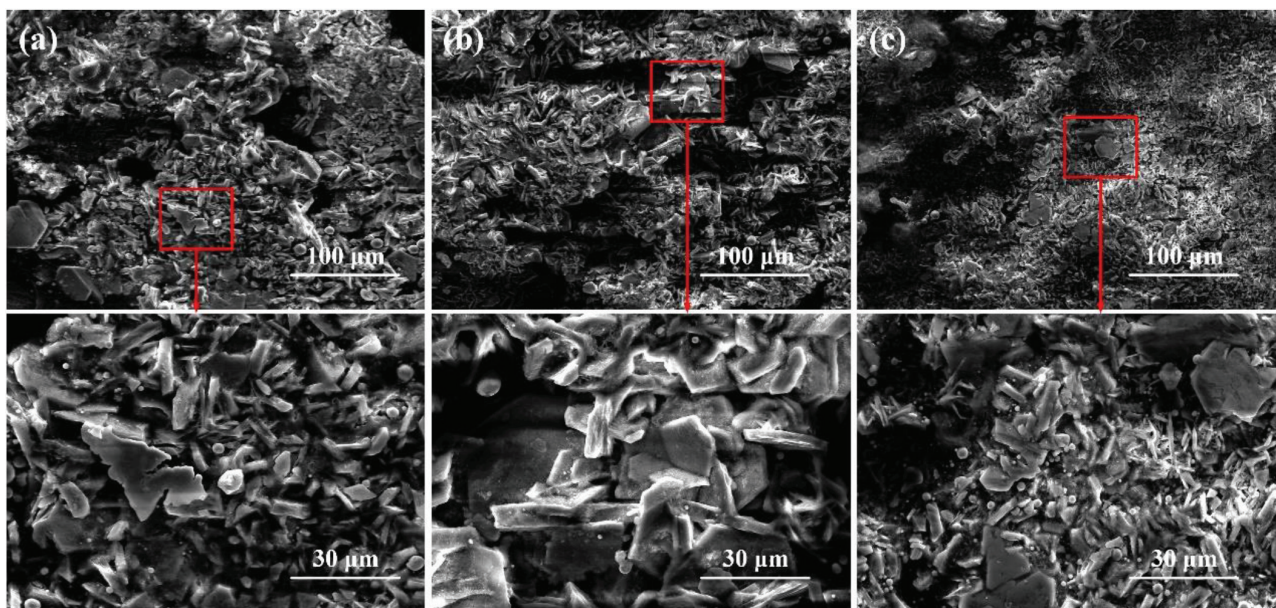


Figure 3: Microstructure of a galvanized X80 pipeline steel welded joint in an accelerated corrosion environment for 4 d: a) weld metal, b) heat-affected zone, c) base metal

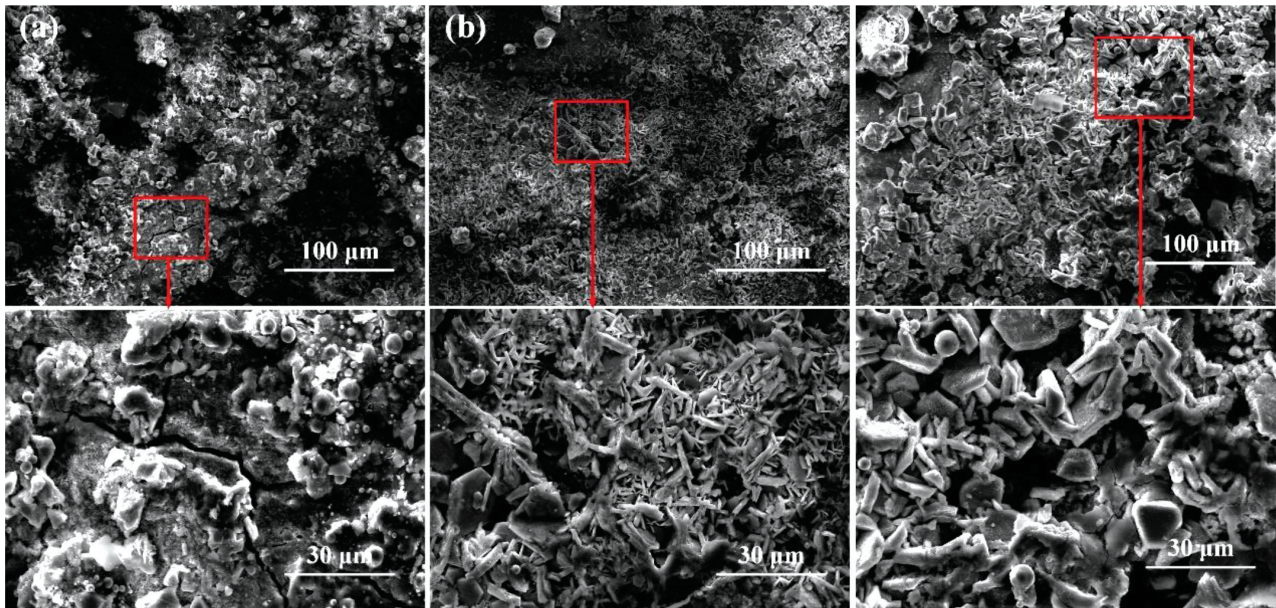


Figure 4: Microstructure of a galvanized X80 pipeline steel welded joint in an accelerated corrosion environment for 8 d: a) weld metal, b) heat-affected zone, c) base metal

and comparing, it can be seen that when exposed for 4 d, the surface of the sample was evenly covered with gray-white corrosion products dominated by the galvanized layer, while other areas retained the original color and luster. When exposed for 8 d, the corrosion products of the coating expanded over the whole surface, which lost its luster, and the corrosion products of the local zinc layer began to fall off. The exposed substrate surface began to corrode and form a brown rust layer, mixed with the corrosion products of the white galvanized layer. When exposed for 16 d, most of the surface of the sample was covered by the brown rust layer. In addition to the loose and easy-to-shed rust layer on the surface, the brown-red rust layer still covered most of the surface, but the local area was still mixed with the white-coating corrosion products. When exposed for 24–40 d, the corrosion products of the coating completely peeled off, and the brown rust layer was regenerated, completely covering the entire surface. As the corrosion time increased, the thickness of the surface rust layer gradually increased and the color gradually deepened. The sampling areas for SEM and EDS are shown in **Figure 3**.

Figure 3 shows the microstructure of a welded joint of galvanized X80 pipeline steel kept in an accelerated corrosion environment for 4 d. It can be seen that the broken zinc layer in the base metal region was relatively flat compared with the HAZ and BM regions, and the whole region had a regular strip shape. The fractured zinc layer plane in the weld area began to accumulate to a certain extent, but the whole area still had a regular lath shape. The broken zinc layer in the heat-affected zone began to accumulate obviously, and the corrosion products were mostly broken zinc layers, showing irregular polygons. At the same time, due to the irregularity of the

corrosion products, there were many pits on the surface of the heat-affected zone.

Figure 4 shows the microstructure of a galvanized X80 pipeline steel welded joint kept in an accelerated corrosion environment for 8 d. It can be seen that the corrosion products on the surface of the entire welded joint were denser than those after 4 d, but they were still dominated by bright galvanized layer corrosion products. The accumulation of corrosion products also began to occur in the base metal area, but the corrosion products on the surface of the base metal still mainly belonged to the zinc layer. The strip-like corrosion products in the weld area were gradually connected to form a dense 'protective layer', but it began to crack in some parts. The zinc layer on the surface of the heat-affected zone represented a dense 'protective layer'. At this time, the zinc layer ruptured more seriously, and the corrosion products were mostly fine needles.

Figure 5 shows the microstructure of a galvanized X80 pipeline steel welded joint kept in an accelerated corrosion environment for 16 d. At this time, the corrosion products of the local galvanized layer began to fall off, and the exposed part of the substrate began to corrode and produce a rust layer, having a mixed and inclusion morphology with the corrosion products of the white coating. The boundary between the zinc layer and the substrate in the weld zone was most obvious because the surface mixed rust layer was loose and cracked, falling off under the action of corrosive media such as Cl⁻. Fine cracks with low brightness began to appear in the matrix. The remaining coating on the surface of the heat-affected zone was evenly distributed across the exposed substrate, but serious cracks appeared. In addition to the local inclusion of white coating corrosion products

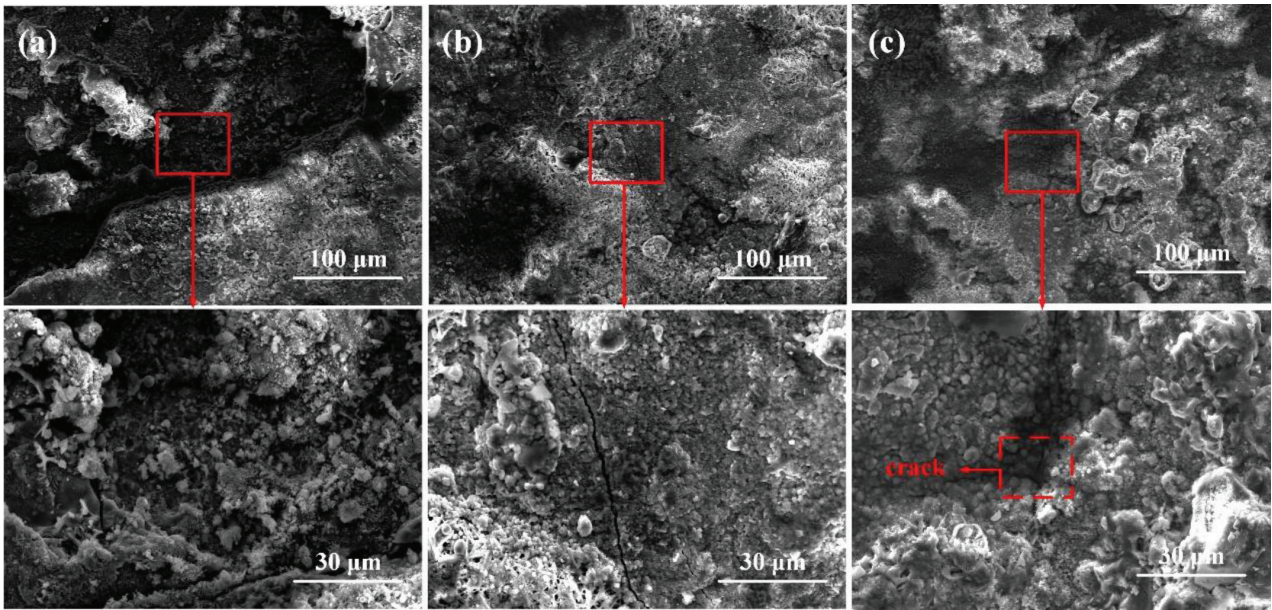


Figure 5: Microstructure of a galvanized X80 pipeline steel welded joint in an accelerated corrosion environment for 16 d: a) weld metal, b) heat-affected zone, c) base metal

in the base metal area, most of the surface was mixed and replaced by the rust layer formed by the corrosion of the substrate, while fine cracks began to appear at the junction.

Figure 6 shows the microstructure of a galvanized X80 pipeline steel welded joint kept in an accelerated corrosion environment for 24 d. When exposed for this period, the corrosion products of the galvanized layer were basically peeled off; the rust layer on the surface of the substrate was regenerated and it expanded across the surface of the whole welded joint. At this time, the gran-

ular corrosion products in the base metal area began to appear and were scattered across the surface. The granular corrosion products in the weld area began to accumulate; at the same time, small cracks began to appear in the rust layer on the surface of the substrate and large cracks appeared in the whole weld area. The granular corrosion products in the heat-affected area were seriously accumulated, and honeycomb dense granular products gradually covered the cracks on the surface.

Figure 7 shows the microstructure of a galvanized X80 pipeline steel welded joint kept in an accelerated

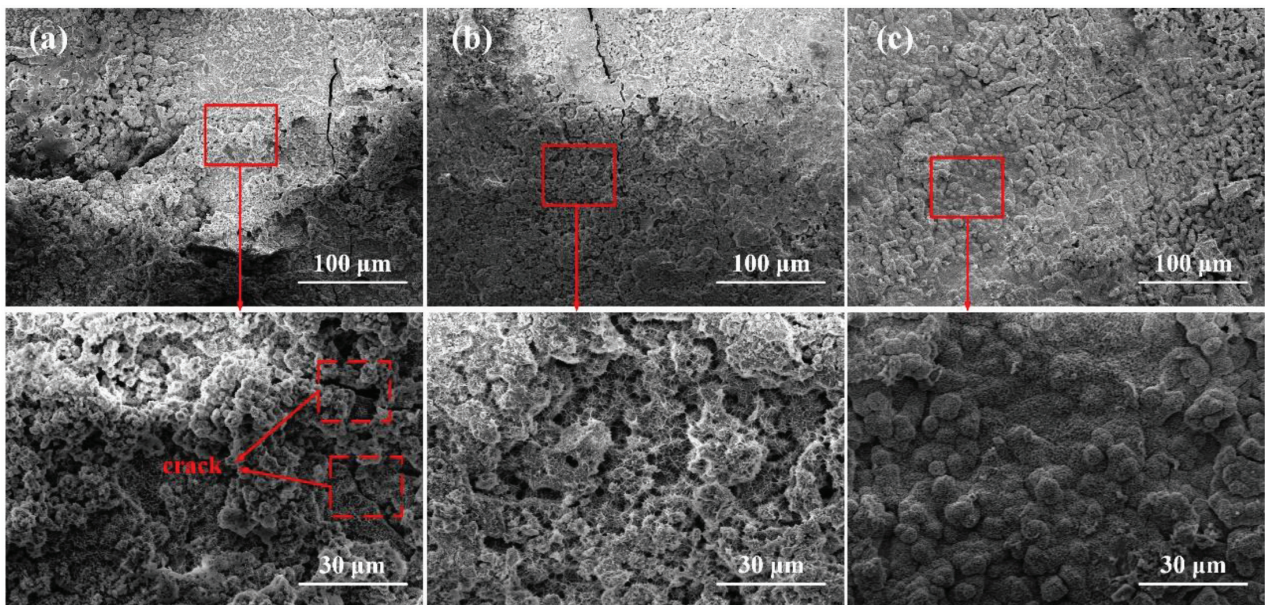


Figure 6: Microstructure of a galvanized X80 pipeline steel welded joint in an accelerated corrosion environment for 24 d: a) weld metal, b) heat-affected zone, c) base metal

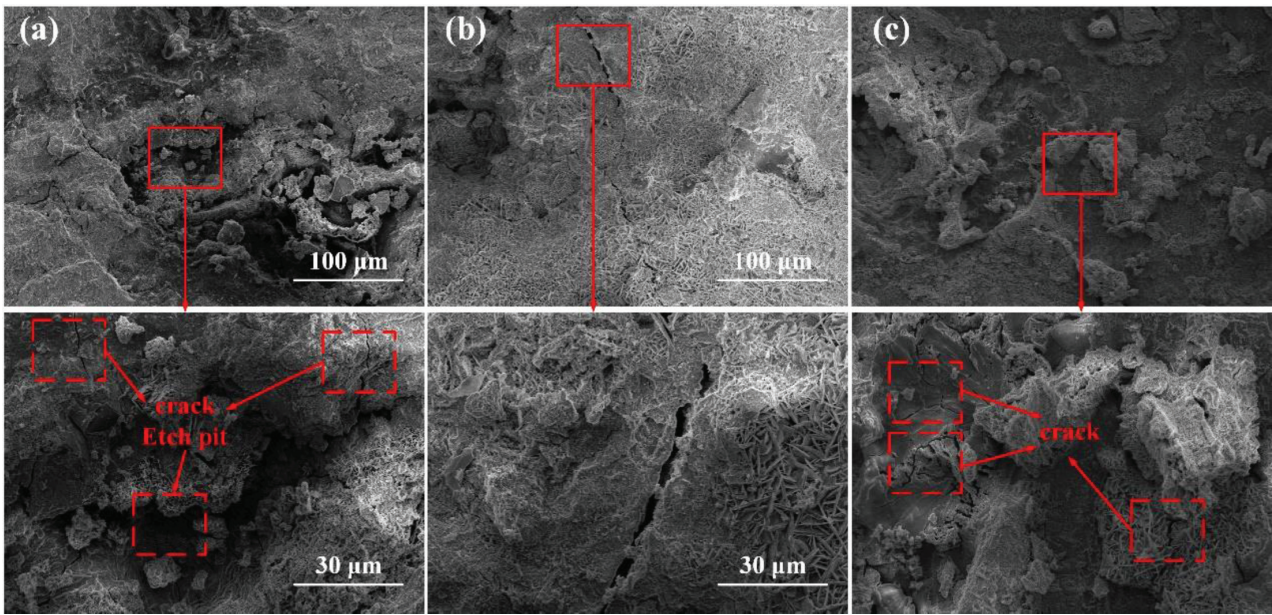


Figure 7: Microstructure of a galvanized X80 pipeline steel welded joint in an accelerated corrosion environment for 32 d: a) weld metal, b) heat affected zone, c) base metal

corrosion environment for 32 d. It can be seen that the accumulation rate of corrosion products in the heat-affected zone was much smaller than the process of rust layer rupture and spalling in this area. Cracks were still there, showing a more serious trend. When exposed for 32 d, the rust layer in the weld area gradually became dense due to the corrosion liquid, penetrating deep into the cracks. Some areas began to show pitting pits, accompanied by small cracks. The corrosion degree of the base metal area was lower than that of the other two areas. Although the accumulation of the surface corrosion products was more serious, only small cracks appeared.

Figure 8 shows the microstructure of a welded joint of galvanized X80 pipeline steel kept in an accelerated corrosion environment for 40 d. At this stage, the pitting corrosion pits at the weld gradually expanded, and the entire weld area was covered with dense pitting corrosion pits. In the heat-affected zone, pitting pits began to appear when cracks still existed and occupied nearly half of the area. The corrosion products in the base metal area began to show regular floccules, and no obvious cracks or pitting pits appeared.

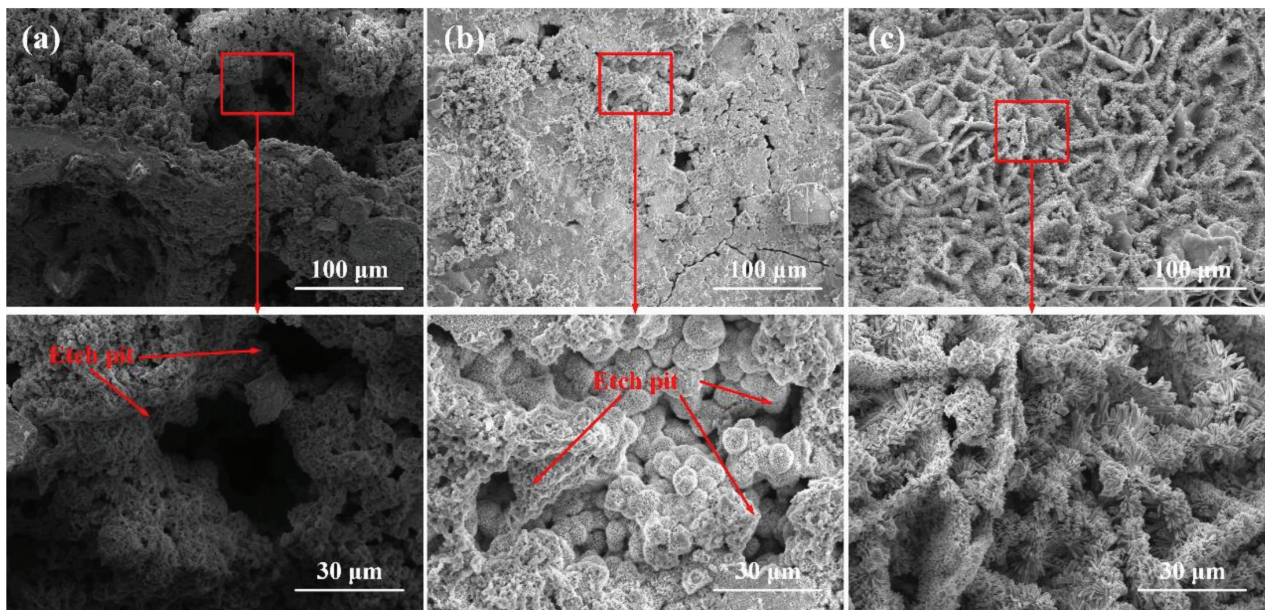


Figure 8: Microstructure of a galvanized X80 pipeline steel welded joint in an accelerated corrosion environment for 40 d: a) weld metal, b) heat affected zone, c) base metal

3.3 Analysis of the corrosion product change

EDS results for corrosion products in different regions of the welded joints of galvanized X80 pipeline steel after exposure to different cycles are shown in **Tables 3, 4** and **5**. From the EDS results and XRD diagrams, it can be seen that the corrosion products generated during the corrosion process gradually transitioned from the galvanized layer to the substrate rust layer. The corrosion products on the surface of the samples exposed for 4–8 d were mainly ZnO. When exposed for 16 d, the corrosion products of the coating fell off locally, and an Fe oxide rust layer of the matrix gradually appeared. When exposed for 24–40 d, the corrosion products of the galvanized layer were basically peeled off and replaced by the rust layer, and the content of Fe gradually increased with the increase in the thickness of the rust layer. In addition, the corrosion products contained certain amounts of Cl, Na and other elements, mainly due to the deposition of the salt solution sprayed during the test.

Table 3: Elements of corrosion products in the weld zone of a galvanized X80 pipeline steel welded joint in w/%

| Exposure time/d | O | Fe | Zn | Cl | Na |
|-----------------|-------|-------|-------|-------|------|
| 4 | 24.32 | 3.43 | 68.93 | 1.64 | 1.70 |
| 8 | 37.83 | 3.51 | 47.13 | 11.53 | – |
| 16 | 42.08 | 12.35 | 45.12 | 0.36 | 1.10 |
| 24 | 22.56 | 61.61 | 13.93 | 1.90 | – |
| 32 | 0.93 | 95.73 | 1.48 | 1.86 | – |
| 40 | 0.31 | 99.30 | 0.37 | 0.02 | – |

Table 4: Elements of corrosion products in the heat-affected zone of a galvanized X80 pipeline steel welded joint in w/%

| Exposure time/d | O | Fe | Zn | Cl | Na |
|-----------------|-------|-------|-------|-------|------|
| 4 | 20.96 | 4.37 | 62.20 | 11.52 | 0.95 |
| 8 | 19.09 | 3.04 | 64.13 | 13.66 | 0.09 |
| 16 | 15.04 | 14.04 | 63.95 | 6.95 | 0.02 |
| 24 | 33.69 | 54.29 | 7.97 | 4.04 | – |
| 32 | 3.59 | 94.82 | 0.42 | 1.17 | – |
| 40 | – | 99.60 | 0.40 | – | – |

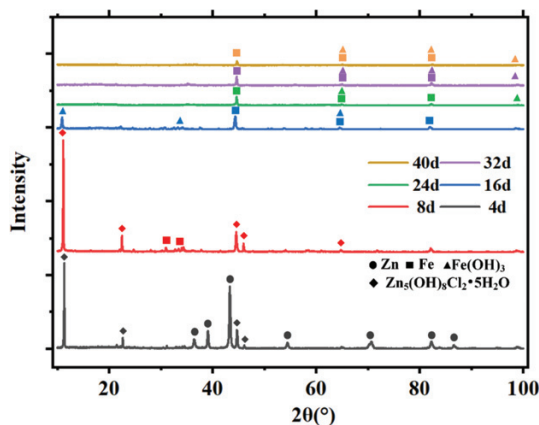


Figure 9: XRD results for corrosion products of galvanized X80 pipeline steel welded joints exposed for different times

Table 5: Elements of corrosion products in the base metal area of a galvanized X80 pipeline steel welded joint in w/%

| Exposure time/d | O | Fe | Zn | Cl | Na |
|-----------------|-------|-------|-------|-------|------|
| 4 | 22.54 | 5.70 | 58.20 | 12.72 | 0.83 |
| 8 | 28.24 | 5.55 | 39.73 | 6.78 | 0.79 |
| 16 | 28.66 | 11.04 | 48.09 | 12.21 | – |
| 24 | 7.12 | 73.53 | 17.73 | 1.62 | – |
| 32 | 23.09 | 72.35 | 0.40 | 4.15 | – |
| 40 | 4.5 | 94.06 | 0.33 | 1.11 | – |

4 CONCLUSIONS

1) The corrosion rate of a galvanized X80 pipeline steel welded joint increases slowly at first and then increases extremely. In the early stage of corrosion, due to the protection of the zinc coating on the substrate, the trend of the corrosion weight loss and corrosion rate increase slowly. In the middle stage of corrosion, the corrosion products produced on the exposed substrate are combined with the corrosion products of the galvanized layer, providing better protection. In the later stage of corrosion, the galvanized layer on the surface of the substrate peels off completely and its protection is lost. The surface of the substrate is affected by corrosive media such as Cl and H⁺, resulting in a rapid increase in the corrosion weight loss and corrosion rate.

2) The corrosion change made to the galvanized X80 pipeline steel welded joint includes the following processes: the formation of galvanized layer corrosion products; local spalling – galvanized layer corrosion products basically spall; matrix rust layer formation – galvanized, matrix, corrosion-product, mixed-matrix, rust-layer growth; and gradual thickening over the entire sample surface.

3) After 8 d of exposure, the zinc layer in the weld metal begins to crack, and it begins to lose its protection of the matrix, thus reducing the corrosion resistance. The corrosive liquid is in direct contact with the matrix after the crack is penetrated, which accelerates the reaction rate, resulting in the first occurrence of pitting pits in the weld metal after 32 d of exposure. When exposed for 16 d, cracks appear in the base metal and heat-affected zone at the same time. However, compared with the narrow and obvious cracks in the heat-affected zone, the cracks in the base metal are almost invisible. Therefore, after the same exposure time, the base metal shows better corrosion resistance. In the early stage of corrosion, the corrosion degree of the zinc layer in the heat-affected zone is more serious than that in the other two regions. And due to an irregular accumulation of corrosion products, there are many pits on the surface. This leads to an accumulation of the corrosive medium in the middle stage of corrosion, so cracks and pitting pits in the heat-affected zone also appear early.

Acknowledgment

This work was supported by the S&P Program of Hebei (Grant No. 22281802Z), and also by the Tangshan Talent Foundation Innovation Team (20130204D), as well as the Science and Technology Project of the Hebei Education Department (QN2021117).

5 REFERENCES

- ¹ X. Qi, P. Huan, X. Wang, et al., Effect of root welding heat input on microstructure evolution and fracture mechanism in intercritically re-heat-coarse grained heat-affected zone of X80 pipeline steel, *Materials Today Communications*, 31 (2022), 103413, doi:10.1016/j.mtcomm.2022.103413
- ² X. Chen, H. Lu, G. Chen, et al., A comparison between fracture toughness at different locations of longitudinal submerged arc welded and spiral submerged arc welded joints of API X80 pipeline steels, *Engineering Fracture Mechanics*, 148 (2015), 110–21, doi:10.1016/j.engfracmech.2015.09.003
- ³ Y. Sun, Y. Frank Cheng, Hydrogen permeation and distribution at a high-strength X80 steel weld under stressing conditions and the implication on pipeline failure, *International Journal of Hydrogen Energy*, 46 (2021) 44, 23100–12, doi:10.1016/j.ijhydene.2021.04.115
- ⁴ X. Li, D. Zhang, Z. Liu, et al., Materials science: Share corrosion data, *Nature*, 527 (2015), 441–2
- ⁵ C. Liu, Z. Li, B. Zhao, et al., Stress corrosion mechanism and susceptibility of X80 steel under a disbonded coating in an acidic soil solution, *Journal of Materials Research and Technology*, 14 (2021), 533–47, doi:10.1016/j.jmrt.2021.06.092
- ⁶ X. Qi, P. Huan, X. Chen, et al., Corrosion resistance and mechanism of X100 pipeline steel laser-metal active gas hybrid welds with Cr containing welding wire in NS4 solution, *Corrosion Science*, 221 (2023), 111329, doi:10.1016/j.corsci.2023.111329
- ⁷ I. A. Chaves, R. E. Melchers, Pitting corrosion in pipeline steel weld zones, *Corrosion Science*, 53 (2011) 12, 4026–32, doi:10.1016/j.corsci.2011.08.005
- ⁸ R. Ashari, A. Eslami, M. Shamanian, et al., Effect of weld heat input on corrosion of dissimilar welded pipeline steels under simulated coating disbondment protected by cathodic protection, *Journal of Materials Research and Technology*, 9 (2020) 2, 2136–45, doi:10.1016/j.jmrt.2019.12.044
- ⁹ D. Persson, D. Thierry, O. Karlsson, Corrosion and corrosion products of hot dipped galvanized steel during long term atmospheric exposure at different sites world-wide, *Corrosion Science*, 126 (2017), 152–65, doi:10.1016/j.corsci.2017.06.025
- ¹⁰ D. Nakhaie, A. Kosari, J. M. C. Mol, et al. Corrosion resistance of hot-dip galvanized steel in simulated soil solution: A factorial design and pit chemistry study, *Corrosion Science*, 164 (2020), doi:10.1016/j.corsci.2019.108310
- ¹¹ M. Yan, B. Wei, J. Xu, et al., Insight into sulfate-reducing bacteria corrosion behavior of X80 pipeline steel welded joint in a soil solution, *Journal of Materials Research and Technology*, 24 (2023), 5839–63, doi:10.1016/j.jmrt.2023.04.163
- ¹² Y. Yan, H. Deng, W. Xiao, et al., Corrosion behaviour of X80 pipeline steel welded joint in H₂O-saturated supercritical-CO₂ environment, *International Journal of Electrochemical Science*, 15 (2020) 2, 1713–26, doi:10.20964/2020.02.38
- ¹³ L. Wang, X. Wang, Z. Cui, et al., Effect of alternating voltage on corrosion of X80 and X100 steels in a chloride containing solution – Investigated by AC voltammetry technique, *Corrosion Science*, 86 (2014), 213–22, doi:10.1016/j.corsci.2014.05.012
- ¹⁴ X. Zhu, J. Chen, Y. Du, Limit load prediction analysis of X80 pipeline containing corrosion in mountainous landslide section, *Geoenvironment Science and Engineering*, 229 (2023), 212107, doi:10.1016/j.geoen.2023.212107
- ¹⁵ I. S. Cole, W. D. Ganther, S. A. Furman, et al., Pitting of zinc: Observations on atmospheric corrosion in tropical countries, *Corrosion Science*, 52 (2010) 3, 848–58, doi:10.1016/j.corsci.2009.11.002
- ¹⁶ S. Wang, K. Luo, T. Sun, et al., Corrosion behavior and failure mechanism of electromagnetic pulse welded joints between galvanized steel and aluminum alloy sheets, *Journal of Manufacturing Processes*, 64 (2021), 937–47, doi:10.1016/j.jmapro.2021.02.039